



HAL
open science

Relation between occurrence probability of freak waves and kurtosis/skewness in unidirectional wave trains under single-peak spectra

Lei Wang, Binzhen Zhou, Peng Jin, Jinxuan Li, Shuxue Liu, Guillaume Ducrozet

► To cite this version:

Lei Wang, Binzhen Zhou, Peng Jin, Jinxuan Li, Shuxue Liu, et al.. Relation between occurrence probability of freak waves and kurtosis/skewness in unidirectional wave trains under single-peak spectra. Ocean Engineering, 2022, 248, pp.110813. 10.1016/j.oceaneng.2022.110813 . hal-03583724

HAL Id: hal-03583724

<https://hal.science/hal-03583724>

Submitted on 22 Feb 2022

HAL is a multi-disciplinary open access archive for the deposit and dissemination of scientific research documents, whether they are published or not. The documents may come from teaching and research institutions in France or abroad, or from public or private research centers.

L'archive ouverte pluridisciplinaire **HAL**, est destinée au dépôt et à la diffusion de documents scientifiques de niveau recherche, publiés ou non, émanant des établissements d'enseignement et de recherche français ou étrangers, des laboratoires publics ou privés.

Relation between occurrence probability of freak waves and kurtosis/skewness in unidirectional wave trains under single-peak spectra

Lei Wang^{a,c,d}, Binzhen Zhou^{a,*}, Peng Jin^{b,**}, Jinxuan Li^c, Shuxue Liu^c, Guillaume Ducrozet^d

^a School of Civil Engineering and Transportation, South China University of Technology, Guangzhou 510641, China

^b School of Marine Science and Engineering, South China University of Technology, Guangzhou 510641, China

^c State Key Laboratory of Coastal and Offshore Engineering, Dalian University of Technology, Dalian 116024, China

^d Ecole Centrale de Nantes, LHEEA Lab (ECN and CNRS), Nantes, France

Abstract

An accurate prediction about the occurrence probability of freak waves in unidirectional wave trains is crucial for avoiding disasters and losses in marine operations. Based on a two-dimensional High Order Spectral numerical wave tank, here the quantitative relation between the occurrence probability of freak waves and kurtosis/skewness considering the influence of Benjamin-Feir Index and relative water depth is investigated. A wide range of 25 single-peak spectral waves is simulated for data collection and further statistical analysis. Results show that the correlation between the occurrence probability of freak waves and skewness depends on the Benjamin-Feir Index and no uniform linear relation is deduced. In contrast, the occurrence probability of freak waves has a strong correlation with kurtosis, irrespective of Benjamin-Feir Index, relative water depth, and peak enhancement factor. An empirical formula for the occurrence probability of freak waves is obtained: $P_{freak}(\%)=0.29kurtosis-0.8$, a little deviation from the one based on the Modified Edgeworth-Rayleigh (MER) weakly nonlinear model.

Keywords: Unidirectional random waves, occurrence probability of freak waves, kurtosis, skewness, single-peak spectra, High Order Spectral method

1. Introduction

Freak waves [1-3] have been reported as a major cause of disasters in the increasing marine development activities [4-7]. It is important to predict the occurrence of freak waves and avoid the latent threat to the safety of offshore structures, ships, and personnel [2, 8, 9]. Owing to the complexity in the onset mechanisms and conditions and randomness, the prediction of a single freak wave event is quite difficult. A more instructional indicator for practical operation is the occurrence probability of freak waves in a prescribed region.

* Corresponding author

E-mail address: zhoubinzhen@scut.edu.cn (B.Z. Zhou)

** Corresponding author

E-mail address: jinpeng@scut.edu.cn (P. Jin)

The probabilistic nature of unidirectional random wave trains could be characterized by kurtosis and skewness. Onorato [10, 11] pointed out that kurtosis could indicate the presence of extreme events, being a measure of the importance of the distribution tail. Whereas, according to Onorato et al. [12], the role of skewness in the wave height distribution is less important compared with kurtosis, because skewness usually comes as a result of second-order corrections and is slightly affected by free wave dynamics. Mori and Janssen [13] discussed the relation between kurtosis and the exceedance probability of wave heights and developed a modified Edgeworth-Rayleigh distribution (MER) by introducing kurtosis in the distribution function under the assumption of weak nonlinearity. Mori et al. [14] confirmed that the nonlinear correction to the maximum wave height depends on kurtosis and the tail of the wave height distribution increases as kurtosis increases. Tayfun and Fedele [15] reviewed theoretical crest-to-trough height distributions and compared them with field data gathered in the North Sea. They found that most linear models yield reasonable predictions similar to the observed data in directional wave trains.

A large amount of long-time observations on individual events are required to deduce an empirical relation between the occurrence probability of freak waves and kurtosis/skewness. Sensors deployed in sites are hardly used for collecting data because of the rarity of freak waves in a relatively confined region. Besides, considering the limits of physical experiments in test conditions and high cost, numerical simulation is widely accepted. There are two possibilities for nonlinear numerical modeling, potential flow theory and Navier-Stokes equation. A Computational Fluid Dynamics (CFD) model requires a very fine grid and consequently high computational effort to propagate waves accurately. The inversion process of the full matrix in the Boundary Element Method (BEM) solver is complex and requires a large amount of calculation. In contrast, the fully nonlinear model based on High Order Spectral (HOS) method has obvious advantages in efficiency.

HOS method was first proposed by Dommermuth and Yue [16] and West et al. [17] to solve the time evolution of a wave field limited to an infinite homogeneous spatial domain. Unlike other classic discretization schemes, the core point of HOS method is to discretize in wavenumber space and truncate to a specific order (known as the nonlinear order of HOS model) according to the calculation requirements. Bonnefoy et al. [18] extended the original HOS method and overcame the limit in the treatment of wavemaker boundary condition by adding an additional velocity potential function. Ducroz et al. [19] enhanced this model to represent a water wave tank, including a wavemaker and an absorbing beach. The advanced HOS numerical wave tank can simulate random wave trains fast and accurately.

To the best of the authors' knowledge, most predictions on the quantitative relation between the occurrence probability of freak waves and kurtosis/skewness are based on a linear or weakly nonlinear model such as MER. A model based on a fully nonlinear method is not available, although strong nonlinearity of freak waves has been observed in many laboratory and field tests. This study is proposed to bridge this gap. The novelties are three-folded. First, HOS method is employed as a tool in collecting data to reflect the full nonlinearity of freak waves. Second, the influences of the Benjamin-Feir Index (BFI) and relative water depth on the relation between occurrence probability and kurtosis/skewness are investigated. Third, an empirical formula of the occurrence probability of freak waves with respect to kurtosis is given.

The rest of the paper is arranged as follows. Section 2 describes the set-up of HOS numerical wave tank, unidirectional random wave conditions, and definitions of key parameters. Section 3 compares the wave height distribution obtained from HOS and MER. Section 4 investigates the relation between

the occurrence probability of freak waves and kurtosis/skewness. An empirical formula for this relation in unidirectional random wave trains under single-peak spectra is deduced, providing a reference for risk vigilance in marine activities.

2. Numerical set-up and data analysis

2.1 Numerical model

A numerical wave tank based on HOS method including a wavemaker and an absorbing beach is adopted to simulate two-dimensional random waves (Figure 1). The initial conditions represent the fluid at rest and the waves are generated with a time-varying boundary condition. The wave tank has constant water depth h and horizontal length L_x .

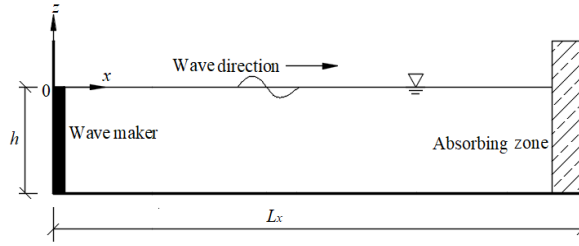


Figure 1. Sketch of the numerical wave tank

Based on the potential flow theory, the numerical solution is achieved with the velocity potential being split into the sum of a free-surface spectral potential component Φ_f and a prescribed non-periodic component Φ_w . The free-surface spectral potential component Φ_f satisfies the Laplace equation, the free surface boundary conditions, and the bottom condition. It can be solved using the original HOS method in which the velocity potential is written in a perturbation series up to an arbitrary order. The free surface boundary conditions are modified with the non-periodic component acting as forcing terms. This additional velocity potential Φ_w satisfies the Laplace equation, the wavemaker boundary condition, and the bottom condition, which can be expressed on another set of specific basis functions concerning a given number of modes. More details of the numerical tank could be referred to Li and Liu [20].

2.2 Irregular wave conditions

The wave maker's motion is determined by the target free surface elevation and the linear transfer function, which depends on its geometry. The target free surface elevation can be represented as a superposition of regular wave components with different frequencies. The wave amplitude of each component is defined from the frequency spectrum $S(\omega)$, proposed by Ochi and Hubble in Ref. [21]:

$$S(\omega) = \frac{1}{4} \frac{\left(\frac{4\lambda + 1}{4}\right)^2}{\Gamma(\lambda)} \left(\frac{\omega_p}{\omega}\right)^{4\lambda} \frac{H_s^2}{\omega} \exp\left[-\frac{4\lambda + 1}{4} \left(\frac{\omega_p}{\omega}\right)^4\right] \quad (1)$$

where Γ is the gamma function. H_s , ω_p , and λ are the significant wave height, the spectral peak angular frequency ($=2\pi f_p$), and the peak enhancement factor, respectively.

Here, the deep-water Benjamin-Feir Index (BFI) used to measure the instability of deep-water waves adopts the definition in Onorato et al.[10, 11]:

$$\text{BFI} = \frac{\sqrt{2\varepsilon}}{2\Delta f / f_p} \quad (2)$$

where $\varepsilon = k_p H_s / 2$ is the wave steepness. The relative spectral bandwidth $\Delta f / f_p$ refers to the definition introduced in Ref. [22]. The values are listed in Table 1.

Table 1. The relation between λ and relative spectral bandwidth

λ	$\Delta f / f_p$
8.0	0.1033
12.0	0.0850
16.0	0.0712

25 cases in the deepwater regime ($k_p h > 3$) listed in Table 2 are designed to study the occurrence probability of freak waves in unidirectional wave trains under single-peak spectra. Among them, Case 1, Case 2, and Case 3 have the same peak enhancement factor but different peak frequencies (i.e., relative water depth $k_p h$), whereas Case 2, Case 4, and Case 5 have the same peak frequency but different peak enhancement factors. In each case, BFI has five different values of 0.2, 0.4, 0.6, 0.8 and 1.0. Detailed parameters of various cases under single-peak spectra are listed in Table 2.

Table 2. Detailed parameters of various cases under single-peak spectra ($h = 4.0\text{m}$)

Case	f_p (Hz)	k_p (m^{-1})	h/L_p	$k_p h$	H_s (m)	$\varepsilon =$ $k_p H_s / 2$	λ	$\Delta f / f_p$	BFI
Case 1	Case 1_a	0.6	1.44	0.92	5.80	0.0278	16	0.071	0.2
	Case 1_b					0.0556			0.4
	Case 1_c					0.0834			0.6
	Case 1_d					0.1112			0.8
	Case 1_e					0.1390			1.0
Case 2	Case 2_a	0.8	2.58	1.64	10.30	0.0156	16	0.071	0.2
	Case 2_b					0.0313			0.4
	Case 2_c					0.0469			0.6
	Case 2_d					0.0625			0.8
	Case 2_e					0.0782			1.0
Case 3	Case 3_a	1.0	4.02	2.56	16.10	0.010	16	0.071	0.2
	Case 3_b					0.020			0.4
	Case 3_c					0.030			0.6
	Case 3_d					0.040			0.8
	Case 3_e					0.050			1.0
Case 4	Case 4_a	0.8	2.58	1.64	10.30	0.0187	12	0.085	0.2
	Case 4_b					0.0373			0.4
	Case 4_c					0.0560			0.6
	Case 4_d					0.0747			0.8
	Case 4_e					0.0934			1.0
Case 5	Case 5_a	0.8	2.58	1.64	10.30	0.0227	8	0.103	0.2
	Case 5_b					0.0454			0.4
	Case 5_c					0.0681			0.6
	Case 5_d					0.0908			0.8
	Case 5_e					0.1135			1.0

2.3 Numerical set-up

In all cases, the total number of wave components describing the temporal wavemaker motion is 200 and the frequency range is (0.2Hz, 3.0Hz). With respect to the discretization in space, the number of points per peak wavelength is 30, the time step is 1/100 of the wave period, and the order of HOS method is 5, referring to the convergence analysis in Ref. [22].

To ensure that the random waves evolve over a sufficiently long extent in space, the numerical wave tank is at least 50 times the corresponding peak wavelength. Therefore, the effective length of the

numerical wave tank is 220 m, 120 m, and 100 m corresponding to the peak frequencies of 0.6 Hz (Case 1), 0.8 Hz (Case 2, 4, 5), and 1.0 Hz (Case 3). The water depth is 4.0 m.

Convergence analysis and validation of this numerical model have been conducted in Ref. [22], demonstrating the accuracy of the HOS numerical wave tank. For more details of the present implementation and the choice of parameters, readers can refer to Ref. [22].

2.4 Data analysis

To obtain sufficiently stable statistics at each fixed location, a large number of waves have been recorded. Ten different random seeds at each location are used to prevent the reflection due to the long-time simulation. The effective simulation time of each seed is around 650 s. Then there are at least 5000 waves for each configuration.

Statistical parameters of these wave trains, such as wave height distribution, kurtosis, and skewness, are analyzed. Note that the exceedance probability of wave height is counted by the zero up-crossing method in the following statistics.

2.4.1 Exceedance probability of wave height

In Rayleigh distribution, the wave height is regarded as twice the envelope amplitude in a stationary, Gaussian, and extremely narrow banded process [23]:

$$E(H) = \exp\left[-\frac{H^2}{8m_0}\right] \quad (3)$$

where $m_0=H_s/4$ is the zero-order spectral momentum,

Naess [24] derived a linear distribution model for the crest-to-trough wave height in narrow-band wave trains given by:

$$E(H) = \exp\left[-\frac{H^2}{4m_0(1-\rho(\tau/2))}\right] \quad (4)$$

where $\rho(\tau/2)$ is the normalized autocorrelation function of the sea surface elevation when it attains its first minimum. Its asymptotic approximation was given in Boccotti [25].

Considering the effect of nonlinear interaction, Mori and Janssen [13] developed MER under the assumption of weak nonlinearity, narrow spectrum, and wave height twice of wave amplitude, expressed as:

$$E(H) = \exp\left(-\frac{H^2}{8m_0}\right) \left[1 + kurtosis \frac{H^2}{384m_0} \left(\frac{H^2}{m_0} - 16\right)\right] \quad (5)$$

2.4.2 Definition of freak wave occurrence probability

H/H_s is used as the criterion to distinguish freak waves. When $H/H_s \geq 2.0$, it is considered as a freak wave. The corresponding probability is defined as the occurrence probability of freak waves, i.e., P_{freak} (Figure 2). This definition is different from the one used in previous studies [26], which mainly focused on the probability of maximum wave height, i.e., P_m (Figure 2). P_m is highly influenced by the duration of the signal, the zero-crossing period, and the number of seeds. Each analyzed signal is sufficiently long and there are several events past the threshold of $H/H_s=2.0$ so that P_{freak} is accurately evaluated. Further, P_{freak} is given as a percentage to represent the freak wave occurrence probability more intuitively.

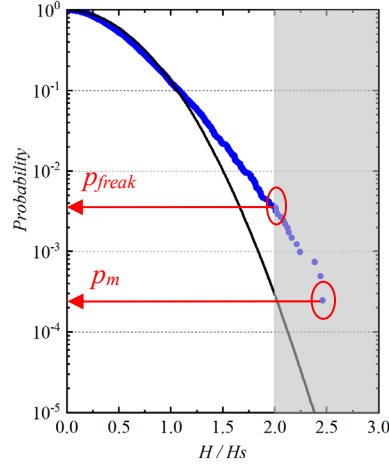


Figure 2. Definition of freak wave occurrence probability

The occurrence probabilities of freak waves in Rayleigh distribution and MER distribution are respectively calculated:

$$\begin{aligned}
 P_{freak-Rayleigh} &= E(H)_{Rayleigh} \Big|_{H=2H_s} \times 100\% \\
 &= EXP \left[-\frac{(2H_s)^2}{8m_0} \right] \times 100\% \\
 &= 0.033\%
 \end{aligned} \tag{6}$$

$$\begin{aligned}
 P_{freak-MER} &= E(H)_{MER} \Big|_{H=2H_s} \times 100\% \\
 &= EXP \left[-\frac{(2H_s)^2}{8m_0} \right] \left(1 + kurtosis \frac{(2H_s)^2}{384m_0} \left(\left(2H_s / \sqrt{m_0} \right)^2 - 16 \right) \right) \times 100\% \\
 &= (0.27kurtosis - 0.77)\%
 \end{aligned} \tag{7}$$

2.4.3 Parameters describing nonlinear statistical characteristics

(a) Kurtosis

Kurtosis of the free surface elevation is defined as:

$$kurtosis = \frac{\langle (\eta - \langle \eta \rangle)^4 \rangle}{\sigma^4} \tag{8}$$

where $\langle \rangle$ represents the average over time and σ is the standard deviation of η .

(b) Skewness

Skewness of the free surface elevation is defined as:

$$skewness = \frac{\langle (\eta - \langle \eta \rangle)^3 \rangle}{\sigma^3} \tag{9}$$

2.4.4 Previous related research

In our previous study [22] (seen in figure 3c), kurtosis evolves along the wave flume with the propagation of waves, as shown in Figure 3. For BFI = 0.2, the kurtosis is almost constant along the wave flume. However, for a larger BFI, kurtosis grows along the wave flume and deviates from the Gaussian value of 3.0. Kurtosis with a larger BFI has a faster growth rate and larger maximum value. When BFI=1.0, the maximum value of kurtosis can reach 4.75. These phenomena can be explained by

modulation instability that depends on the wave steepness and spectral bandwidth. Therefore, the statistical characteristics of all different locations that exhibit different kurtosis are needed to be considered in the following study.

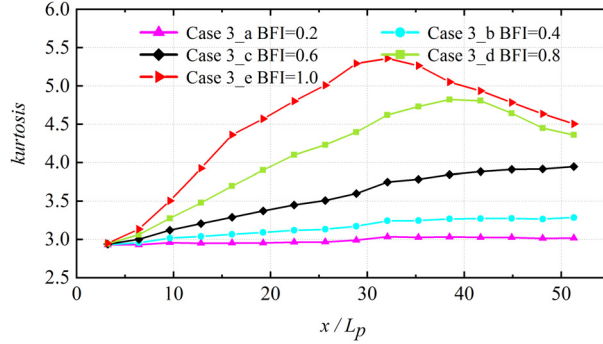


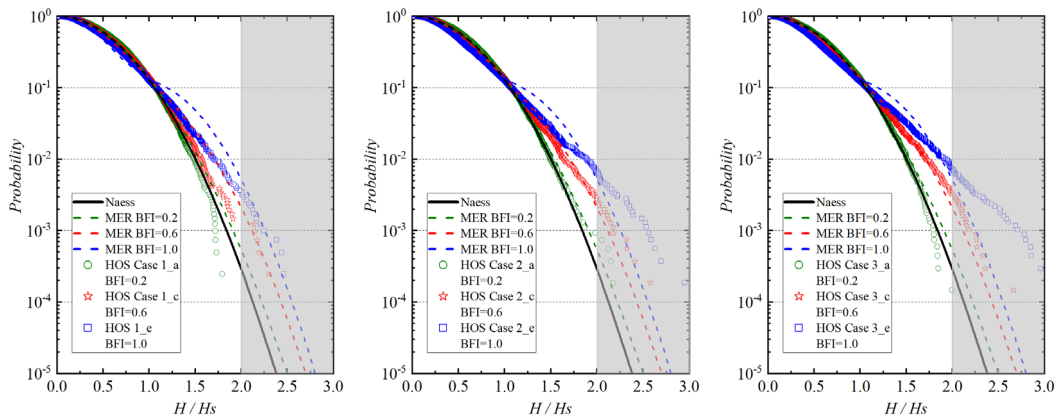
Figure 3. The evolutions of kurtosis for various BFIs under single-peak spectra (Case 3: $k_p h = 16.10$, $\lambda = 16$)

3. Comparison of wave height distribution

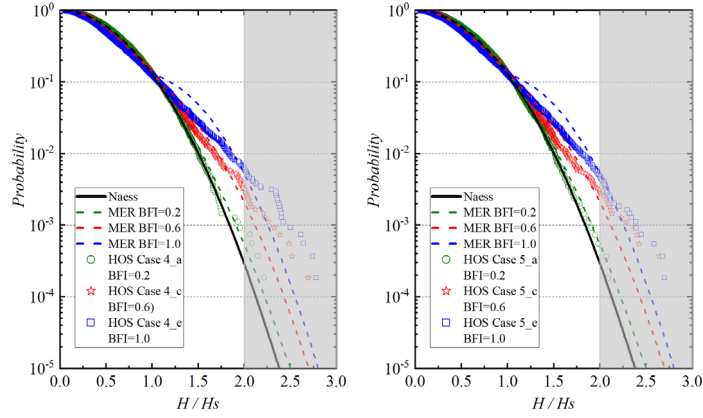
The main effects of BFI, relative water depth $k_p h$, and peak enhancement factor λ on wave height distribution are investigated in this section.

Figure 4 displays the exceedance probabilities of wave height at the location of the maximum kurtosis for various BFIs calculated by HOS method. Naess distribution and corresponding MER distribution are plotted for comparison.

For BFI=0.2, the wave height distribution almost obeys Naess distribution. As BFI increases, the wave height distribution gradually deviates from Naess distribution. A larger BFI leads to a greater probability of large wave height. Both Naess distribution and MER distribution can well predict statistics of wave height distribution when H/H_s is smaller than 1.5. As third-order nonlinearity is considered, MER distribution can better predict the probability of large waves ($1.5 < H/H_s < 2.0$), but underestimates the statistics of the height distribution when H/H_s is larger than 2.0, which is the classic value to identify events are rogue or freak waves [27].



(a) Case 1 ($k_p h = 5.80$, $\lambda = 16$) (b) Case 2 ($k_p h = 10.30$, $\lambda = 16$) (c) Case 3 ($k_p h = 16.10$, $\lambda = 16$)



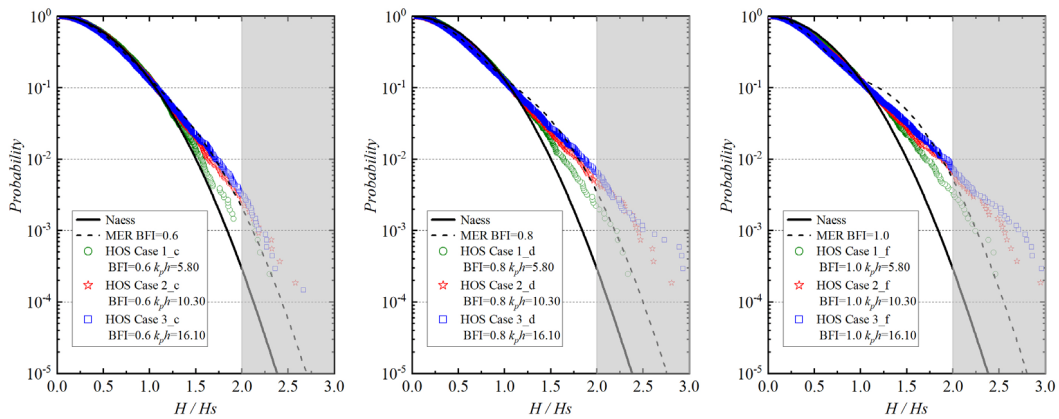
(d) Case 4 ($k_p h=10.30, \lambda=12$) (e) Case 5 ($k_p h=10.30, \lambda=8$)

Figure 4. Exceedance probability of wave height at maximum kurtosis for various BFIs under single-peak spectra for unidirectional waves (black solid lines: Naess distribution, colored dotted lines: MER distribution)

The wave height exceedance probability of random wave trains with the same BFI but various relative water depth $k_p h$ and peak enhancement factor λ is given in Figure 5 and Figure 6, respectively.

In Figure 5, when the BFI is fixed, as the relative water depth $k_p h$ increases, the deviation of wave height distribution from Naess increases. Additionally, with the increase of BFI, the deviation of wave height distribution from Naess becomes greater. These trends indicate that the increase of BFI leads to the enhancement of the nonlinear interaction among wave components and then results in the underestimation of wave height distribution in linear models.

In Figure 6, irrespective of the peak enhancement factor λ , their wave height distributions keep consistent, showing that the relative spectral bandwidth has little effect on the wave height distribution of unidirectional random wave trains with the same initial nonlinear strength (i.e., BFI of input wave spectrum).

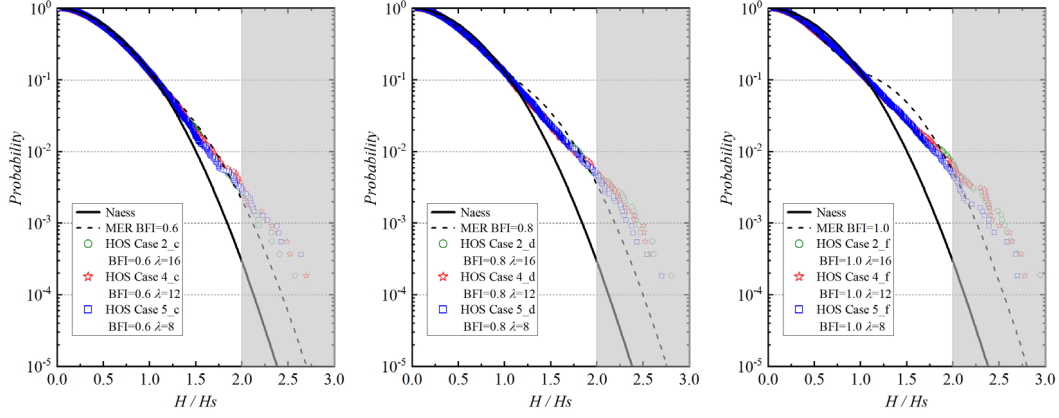


(a) BFI=0.6, $\lambda=16$

(b) BFI=0.8, $\lambda=16$

(c) BFI=1.0, $\lambda=16$

Figure 5. The influence of relative water depth on exceedance probability of wave height at maximum kurtosis under single-peak spectra for unidirectional waves (black solid lines: Naess distribution; black dotted lines: MER distribution)



(d) BFI=0.6, $k_p h=10.30$

(e) BFI=0.8, $k_p h=10.30$

(f) BFI=1.0, $k_p h=10.30$

Figure 6. The influence of peak enhancement factor on exceedance probability of wave height at maximum kurtosis under single-peak spectra for unidirectional waves (black solid lines: Naess distribution; black dotted lines: MER distribution)

MER distribution underpredicts the wave height distribution when $H/H_s \geq 2.0$. This is because the contribution of nonlinearity higher than third-order, which is not involved in MER, cannot be neglected. HOS method is therefore required.

4. Occurrence probability of freak waves

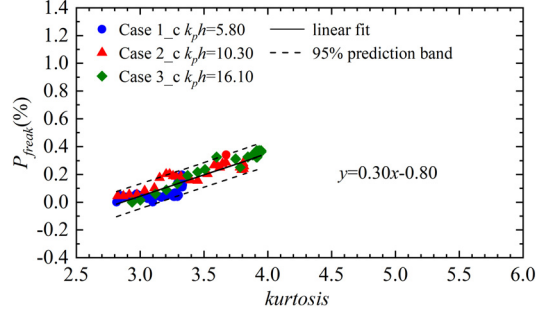
In this section, the influences of BFI and relative water depth $k_p h$ are investigated. The empirical relation between the freak wave occurrence probability P_{freak} and kurtosis/skewness in single-peak spectral unidirectional wave trains are derived.

4.1 Relation between freak wave occurrence probability and kurtosis

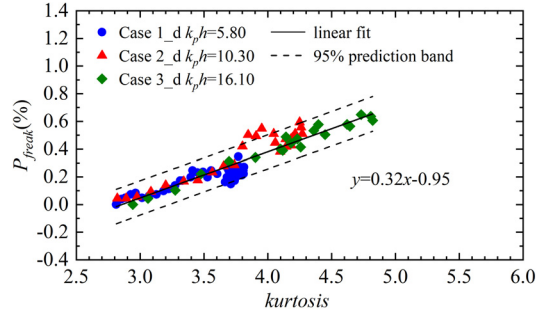
4.1.1 Influence of BFI

Figure 7 displays the influence of BFI on the relation between the occurrence probability of freak waves P_{freak} and kurtosis. From Figure 7(a) (b) and (c), when BFI and peak enhancement factor λ are constant, as the relative water depth $k_p h$ increases, the deviation of kurtosis from 3.0, the maximum kurtosis, and the maximum freak wave occurrence probability P_{freak} become uniformly larger. And cases with larger BFI have larger maximum kurtosis and larger freak wave occurrence probability P_{freak} .

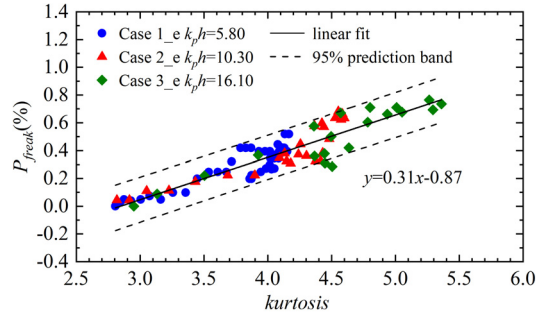
For a fixed BFI, irrespective of the peak enhancement factor λ , the occurrence probability of freak waves P_{freak} increases linearly with kurtosis. For different BFIs, the slope of which the occurrence probability of freak waves P_{freak} increases with kurtosis remains almost unchanged, indicating that BFI has little effect on the growth rate.



(a) BFI=0.6, $\lambda=16$



(b) BFI=0.8, $\lambda=16$



(c) BFI=1.0, $\lambda=16$

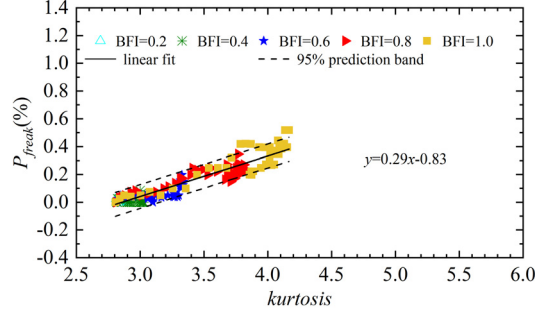
Figure 7. Influence of BFI on the relation between occurrence probability of freak waves P_{freak} and kurtosis under single-peak spectra in unidirectional wave trains.

4.1.2 Influence of relative water depth

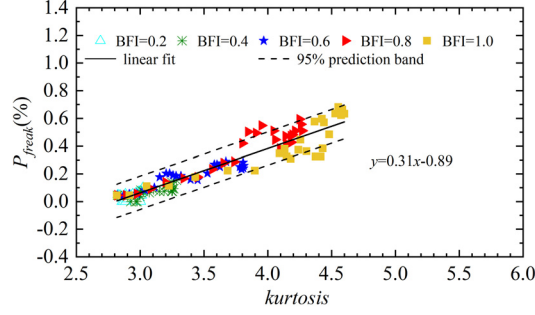
The influence of relative water depth $k_p h$ on the relation between occurrence probability of freak waves P_{freak} and kurtosis is investigated, shown in Figure 8.

For BFI=0.2, the kurtosis at different positions along the wave flume is approximate 3.0. The occurrence probability of freak waves P_{freak} is very small. This is mainly because for a wave train with a small initial BFI, its third-order nonlinearity is relatively weak. As a result, the occurrence probability of large waves is very small and the wave height obeys Rayleigh distribution. As BFI increases, kurtosis increases gradually and the occurrence probability of freak waves P_{freak} also becomes larger. This is caused by the increase in the strength of nonlinearity in the initial wave trains.

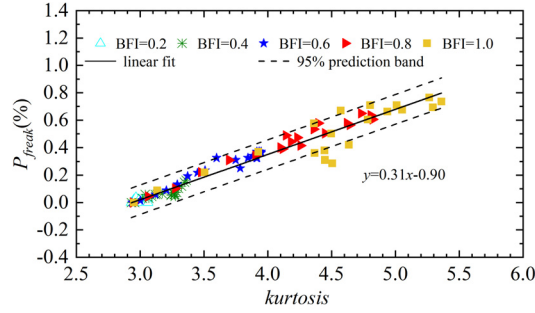
The correlation between the occurrence probability of freak waves P_{freak} and kurtosis is quite obvious, reflected by a positive linear relation. For different relative water depth $k_p h$, the slope of which the occurrence probability of freak waves P_{freak} increases with kurtosis changes little, showing that relative water depth $k_p h$ has little effect on the relation between the occurrence probability of freak waves and kurtosis.



(a) Case 1 ($k_p h = 5.80$, $\lambda = 16$)



(b) Case 2 ($k_p h = 10.30$, $\lambda = 16$)



(c) Case 3 ($k_p h = 16.10$, $\lambda = 16$)

Figure 8. Influence of relative water depth on the relation between occurrence probability of freak waves P_{freak} and kurtosis under single-peak spectra in unidirectional wave trains

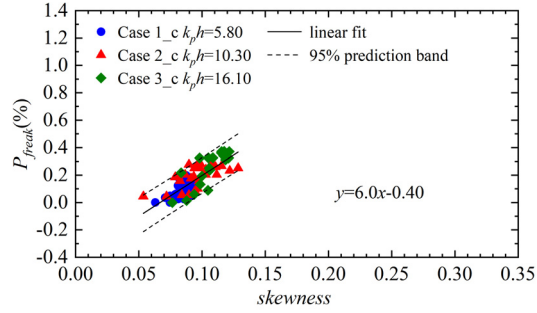
4.2 Relation between freak wave occurrence probability and skewness

Being a measure of wave vertical asymmetry, skewness is expected to be more significant in steep waves and consequently possibly related to freak waves. Therefore, it is of interest to investigate if there is a correlation between the occurrence probability of freak waves and skewness. The influence of BFI on the relation between occurrence probability of freak waves P_{freak} and skewness is analyzed, shown in Figure 9, where (a), (b), and (c) are with the same peak enhancement factor λ but different relative water depth $k_p h$.

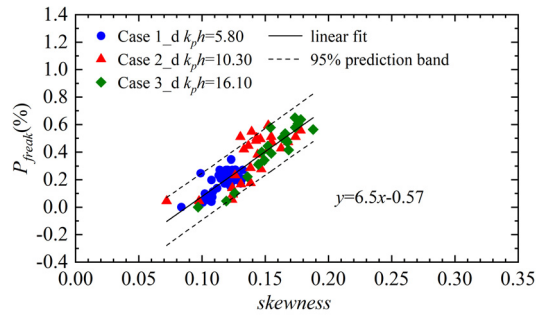
From Figure 9 (a), when BFI and peak enhancement factor λ are constant, the maximum skewness can be reached. The maximum value of the freak wave occurrence probability P_{freak} becomes larger as relative water depth $k_p h$ increases. And cases with larger BFIs (Figure 9 (b) and (c)) have larger maximum skewness and larger occurrence probability of freak waves P_{freak} .

For different BFIs (comparing Figure 9 (a) (b) and (c)), although the occurrence probability of freak waves P_{freak} increases linearly with kurtosis, the slope of which the occurrence probability of freak waves P_{freak} increases with skewness is different. Hence, there is no uniform regression relation

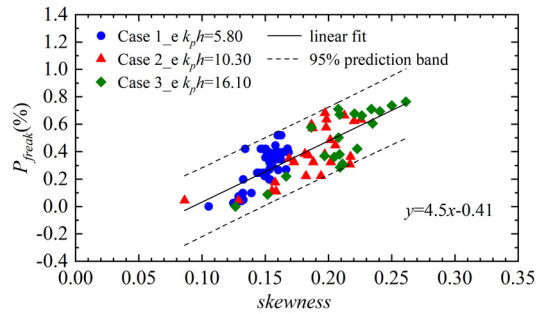
between the occurrence probability of freak waves P_{freak} and skewness for different BFIs, even if it is clear that a higher probability of freak waves is associated with large skewness.



(a) BFI=0.6, $\lambda=16$



(b) BFI=0.8, $\lambda=16$

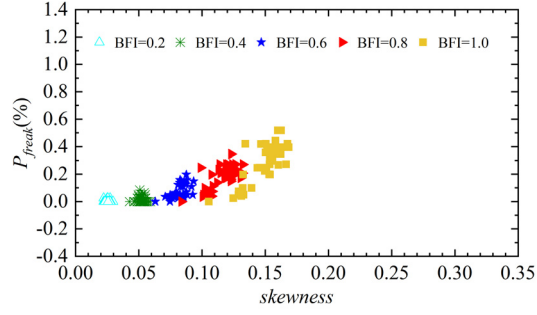


(c) BFI=1.0, $\lambda=16$

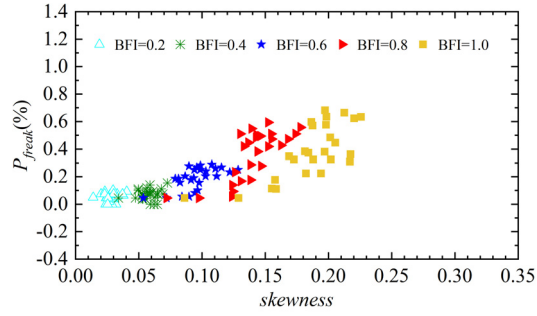
Figure 9. Influence of BFI on the relation between occurrence probability of freak waves P_{freak} and skewness under single-peak spectra in unidirectional wave trains

Figure 10 gives the influence of relative water depth $k_p h$ on the relation between the occurrence probability of freak waves P_{freak} and skewness. For BFI=0.2, skewness is smaller than 0.05, resulting from the weak second-order nonlinear effects in the evolution of the wave trains. As BFI increases, skewness increases gradually and the occurrence probability of freak waves P_{freak} also becomes larger.

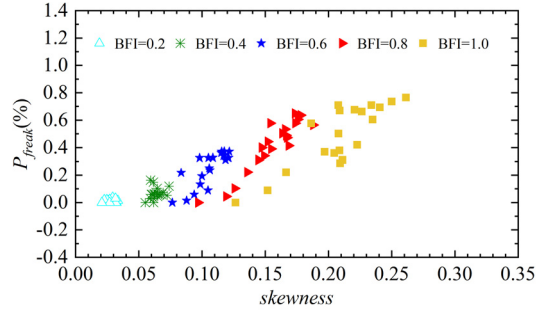
The slope of which the occurrence probability of freak waves P_{freak} depends on BFI and there is no uniform regression relation between the occurrence probability of freak waves P_{freak} and skewness for different relative water depth $k_p h$.



(a) Case 1 ($k_p h = 5.80$, $\lambda = 16$)



(b) Case 2 ($k_p h = 10.30$, $\lambda = 16$)



(c) Case 3 ($k_p h = 16.10$, $\lambda = 16$)

Figure 10. Influence of relative water depth on the relation between occurrence probability of freak waves P_{freak} and skewness under single-peak spectra in unidirectional wave trains

4.3 Empirical formula for freak wave occurrence probability

Based on the above analysis, the empirical formula of the occurrence probability of freak waves P_{freak} with respect to kurtosis is deduced (Figure 11). To eliminate the difference in statistical properties exhibited in different locations of the tank, all wave trains are used. Irrespective of BFI, relative water depth $k_p h$, and peak enhancement factor λ , the occurrence probability of freak waves P_{freak} has a strong correlation with kurtosis, constituting a uniform linear relation, namely:

$$P_{freak} = 0.29kurtosis - 0.82 \quad kurtosis \in (3.0, 5.5) \quad (10)$$

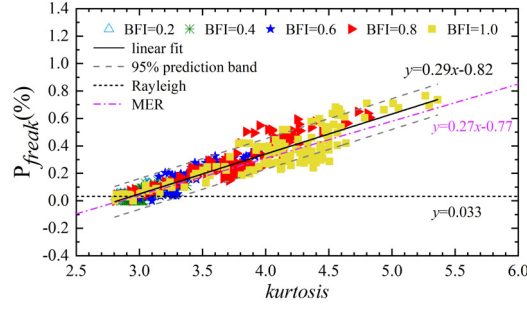


Figure 11. Relation between occurrence probability of freak waves P_{freak} and kurtosis for all cases numerically simulated under single-peak spectra in unidirectional wave trains

Once the wave characteristics of the unidirectional random wave trains under single-peak spectra are known, the maximum kurtosis of the wave trains can be obtained according to the contour plot of the maximum kurtosis with respect to different initial deep-water BFI and the inverse of relative water depth $1/(k_p h)$ [22]. And then through the quantitative relation in Eq. (10), the occurrence probability of freak waves P_{freak} under this wave condition can be predicted.

5. Conclusions

In this paper, the freak wave occurrence probability of unidirectional wave trains under single-peak spectra is investigated from a series of continuous long-time numerical simulations taking full nonlinearities into account in the process based on HOS method.

The exceedance probabilities of wave height for different BFI and relative water depth $k_p h$ obtained from Naess linear model, MER, and HOS numerical results are compared. As BFI and relative water depth $k_p h$ increase, the influence of nonlinearity intensifies. MER gradually becomes invalid and HOS method is required for fully nonlinear simulation, as in the real freak waves.

The relation between the occurrence probability of freak waves and kurtosis/skewness is studied. The correlation between the occurrence probability of freak waves P_{freak} and skewness is heavily influenced by BFI. No uniform linear relation is deduced. The correlation between the occurrence probability of freak waves P_{freak} and kurtosis is irrespective of BFI, relative water depth $k_p h$, and peak enhancement factor λ . A uniform linear relation is obtained as $P_{freak}=0.29kurtosis-0.8$.

Acknowledgments

This work was supported by the National Natural Science Foundation of China (52071096).

References

- [1] M. Onorato, A.R. Osborne, M. Serio, S. Bertone, Freak waves in random oceanic sea states, *Phys Rev Lett* 86(25) (2001) 5831-4.
- [2] C. Kharif, E. Pelinovsky, Physical mechanisms of the rogue wave phenomenon, *European Journal of Mechanics - B/Fluids* 22(6) (2003) 603-634.
- [3] N. Mori, Occurrence probability of a freak wave in a nonlinear wave field, *Ocean Engineering* 31(2) (2004) 165-175.
- [4] M.L. McAllister, T.S. van den Bremer, Lagrangian Measurement of Steep Directionally Spread Ocean Waves: Second-Order Motion of a Wave-Following Measurement Buoy, *Journal of Physical Oceanography* 49(12) (2019) 3087-3108.

- [5] M.L. McAllister, T.S. van den Bremer, Experimental Study of the Statistical Properties of Directionally Spread Ocean Waves Measured by Buoys, *Journal of Physical Oceanography* 50(2) (2020) 399-414.
- [6] M.D. Orzech, D. Wang, Measured Rogue Waves and Their Environment, *Journal of Marine Science and Engineering* 8(11) (2020).
- [7] I. Karpadakis, C. Swan, M. Christou, Assessment of wave height distributions using an extensive field database, *Coastal Engineering* 157 (2020).
- [8] A. Toffoli, J.M. Lefèvre, E. Bitner-Gregersen, J. Monbaliu, Towards the identification of warning criteria: Analysis of a ship accident database, *Applied Ocean Research* 27(6) (2005) 281-291.
- [9] E.M. Bitner-Gregersen, A. Toffoli, Occurrence of rogue sea states and consequences for marine structures, *Ocean Dynamics* 64(10) (2014) 1457-1468.
- [10] M. Onorato, A. Osborne, M. Serio, L. Cavaleri, C. Brandini, C. Stansberg, Observation of strongly non-Gaussian statistics for random sea surface gravity waves, *Phys Rev E* 70(6) (2004) 067302.
- [11] M. Onorato, A. Osborne, M. Serio, Modulational instability and non-Gaussian statistics in experimental, (2005).
- [12] M. Onorato, A.R. Osborne, M. Serio, On Deviations from Gaussian Statistics for Surface Gravity Waves, (2005).
- [13] N. Mori, P.A.E.M. Janssen, On Kurtosis and Occurrence Probability of Freak Waves, *J.phys.oceanogr* 36(7) (2006) 1471-1483.
- [14] N. Mori, M. Onorato, P.A.E.M. Janssen, A.R. Osborne, M. Serio, On the extreme statistics of long-crested deep water waves: Theory and experiments, *Journal of Geophysical Research* 112(C9) (2007).
- [15] M.A. Tayfun, F. Fedele, Wave-height distributions and nonlinear effects, *Ocean Engineering* 34(11-12) (2007) 1631-1649.
- [16] D. Dommermuth, D. Yue, A high-order spectral method for the study of nonlinear gravity waves, 184 (1987) 267-288.
- [17] B.J. West, K.A. Brueckner, R.S. Janda, D.M. Milder, R.L. Milton, A new numerical method for surface hydrodynamics, *Journal of Geophysical Research* 92(C11) (1987).
- [18] F. Bonnefoy, G. Ducrozet, D. Le Touzé, P. Ferrant, Time Domain Simulation of Nonlinear Water Waves Using Spectral Methods, *Advances in Numerical Simulation of Nonlinear Water Waves 2010*, pp. 129-164.
- [19] G. Ducrozet, F. Bonnefoy, D. Le Touzé, P. Ferrant, A modified High-Order Spectral method for wavemaker modeling in a numerical wave tank, *European Journal of Mechanics - B/Fluids* 34 (2012) 19-34.
- [20] J.-x. Li, S.-x. Liu, Focused wave properties based on a high order spectral method with a non-periodic boundary, *China Ocean Engineering* 29(1) (2015) 1-16.
- [21] M. Ochi, E. Hubble, Six parameter wave spectra, 15th International Conference on Coastal Engineering, Honolulu, Hawaii, United States, 1976.
- [22] L. Wang, J. Li, S. Liu, G. Ducrozet, Statistics of long-crested extreme waves in single and mixed sea states, *Ocean Dynamics* 71(1) (2020) 21-42.
- [23] M. Longuet-Higgins, On the statistical distribution of the heights of sea waves, *Journal of Marine Research* 11(3) (1952) 245-266.
- [24] A. Naess, On the distribution of crest to trough wave heights, *Ocean Engineering* 12(3) (1985) 221-234.
- [25] P. Boccotti, *Wave mechanics for ocean engineering*, Oxford: Elsevier Science 2000.
- [26] J.F. Luxmoore, S. Ilic, N. Mori, On kurtosis and extreme waves in crossing directional seas: a laboratory experiment, *Journal of Fluid Mechanics* 876 (2019) 792-817.
- [27] P. Klinting, S. Sand, Analysis of prototype freak waves, *Coastal Hydrodynamics* (1987) 1-15.